Performance evaluation of Welch's periodogram-based energy detection for spectrum sensing

Article *in* IET Communications · July 2013

DOI: 10.1049/iet-com.2012.0640

2 authors:

Daniela Martinez
Autonomous University of Baja California
9 PUBLICATIONS **102** CITATIONS

SEE PROFILE

Ángel G. Andrade
Autonomous University of Baja California
79 PUBLICATIONS **339** CITATIONS

SEE PROFILE

Published in IET Communications
Received on 18th October 2012
Revised on 26th February 2013
Accepted on 24th March 2013
doi: 10.1049/iet-com.2012.0640

ISSN 1751-8628

Performance evaluation of Welch's periodogram-based energy detection for spectrum sensing

Daniela M. Martínez[1], *Ángel G. Andrade*[1]

Engineering School, University of Baja California, Boulevard Benito Juárez s/n, col. Insurgentes, C.P. 21900 Mexicali, Baja California, Mexico
E-mail: daniela.martinez@uabc.edu.mx; aandrade@uabc.edu.mx

Abstract: In this work, the authors present the evaluation of energy detection (ED) based on the Welch's periodogram for spectrum sensing applied to cognitive radio networks. The authors analyse the impact of the number of points in the discrete Fourier transform and the number of averaged periodograms for power density spectrum estimation on the performance of ED. The authors identify that the inclusion of these parameters in the distribution of the test statistic used to detect the presence of primary users, improves the probability of detection. However, in the presence of noise uncertainty, the improvement on the probability of detection will come at the expense of an increased probability of false alarm. With the approach considered in this work is possible to increment the probability of detection for a given and low signal-to-noise ratio, without increasing the number of samples collected from primary signal. However, to maintain a constant probability of false alarm, accurate techniques for noise variance estimation are needed, because detection-threshold value is highly dependent on the noise power present at each sensing interval.

1 Introduction

Recent studies reveal that multiple spectrum bands assigned to licensees (e.g. cellular telephony operators and TV Broadcasters) are underutilised because of the traffic dynamics. As a result, utilisation of radio spectrum reported varies from 2 to 95% [1, 2]. This means that whereas some spectral bands are highly utilised, there are other bands that are idle most part in time and space. This underutilisation of the radio spectrum opens new possible avenues for spectrum accessing to emergent and evolving wireless and mobile systems.

Cognitive radios (CRs) have been proposed as a solution to improve spectrum utilisation by enabling opportunistic spectrum sharing [3]. Their technological capabilities allow CRs to dynamically seek and access to unused portions of the radio spectrum, and thus improving spectrum utilisation. The main requirement for the CRs to make use of spectral opportunities (also called spectrum holes [4]) is to protect primary (licensed) users (PUs) from interference caused by secondary transmissions. In this sense, to opportunistically accessing into temporally and/or spatially unused licensed bands, efficient identification of spectrum holes is required.

Spectrum sensing allows secondary (cognitive) users (SUs) to autonomously identify unused spectrum bands without the need of primary systems intervention. To this time, various methods have been proposed in literature for spectrum sensing. For example, matched filtering is optimal, in the sense that it maximises signal-to-noise ratio (SNR), and therefore minimises detection time. However, synchronisation with primary transmitter is required. Furthermore, it needs dedicated receiver circuitry for every band considered for secondary access, making CR receiver complexity prohibitive [5]. Cyclostationary feature detection has the advantage of distinguishing between noise and primary signals, at the expense of extensive computational requirements. Moreover, it needs exact knowledge of primary signal parameters to correctly identify cyclic frequencies and achieve good performance [6]. Other spectrum sensing techniques are also discussed in [5]. Energy detection (ED) [7] is commonly utilised for detecting the presence of unknown signals, since it does not have strict requirements regarding information 'a priori' about the signal to be detected [8]. However, even though ED is simpler than matched filtering or cyclostationary feature detection, it cannot distinguish when energy comes from PUs' transmissions, interference, or just noise, and therefore its performance is susceptible to noise uncertainty [9]. There are other spectrum sensing techniques that overcome the problem of noise uncertainty without requiring exact knowledge of the parameters regarding the signal monitored, see, for example [10, 11]. Although these techniques perform well under low SNR conditions, they need long observation time and cooperation of a large number of secondary receivers in order to perform near to its optimum.

Commonly ED is implemented in time-domain, in which the incoming signal is filtered, and then passed through a square-law device and an integrator in order to obtain the energy measurement. The energy measured is compared with a predefined threshold to decide if a primary signal is present or not. Although simple, this implementation is

quite inflexible, particularly if the SU needs to sense multiple channels with different characteristic bandwidths (e.g. narrow band or wideband channels) [12].

A different approach is to implement energy (or equivalently power) detection in frequency domain. ED in frequency domain could provide the flexibility to process wider bandwidths and sense multiple channels simultaneously by properly selecting the frequency bins in the discrete representation of the power density spectrum (PDS) [13]. In this approach, an estimate of the PDS is considered to obtain the energy measurement used to decide if a signal is present or not.

Even though there are various methods proposed for PDS estimation (see e.g. [14, chapter 14]), not many of them have been investigated for spectrum sensing in CR networks. In [15], Cabric *et al.* obtain the SNR limit for ED, given sensing time and target performance, by carrying out experimental measurements in an indoor environment with multiple sensing nodes. The energy measurements were obtained in frequency domain by PDS estimation using the well known method of the periodogram [14]. However, their evaluation does not take into account the quality of the PDS estimate on the spectrum sensing performance. In [16], Gismalla and Alsusa determine theoretical performance for the periodogram-based energy detector in fading channels. Their results show that for the detector proposed, the frequency domain approach reduces the probability of false alarm (i.e. deciding that a signal is present when is not) at the cost of reduced detection rate, compared with the time-domain approach. They also mention that whereas the detection rate of the frequency domain approach could be improved by using a variety of techniques such as the Neyman-Pearson criterion, the false alarm rate could not be enhanced any further in time-domain.

In the aforementioned works, authors consider the periodogram method to estimate the PDS of the PU signal, which corresponds to an asymptotically unbiased but non-consistent estimate of the true PDS [14]. In [17], Sarvanko *et al.* generalise theoretical foundations of ED for the case of Welch's periodogram and analyse performance of spectrum sensing in Gaussian channels, concluding that the Welch method for PDS estimation performs better than the periodogram method for detecting narrowband signals. Later in [18], Matinmikko *et al.* extend the study presented in [17] for Rayleigh fading channels. Their results show that detection performance in fading channels is only improved by cooperation among multiple sensing nodes. However in these works, it is not addressed how the method employed for the PDS estimation improves or degrade the performance of spectrum sensing.

Welch proved that by segmenting the data sequence and by letting consecutive data segments to overlap, the average of the resulting periodograms obtained from individual data segments reduces the variance in the PDS estimate, and thereby increases estimate quality [19]. In the context of ED for spectrum sensing, reducing the variability of the PDS estimate, or equivalently increasing its quality, will result in a more reliable estimation of the energy contained in the channel of interest, which is a desirable property of the ED method. However, improving this estimate will not necessarily improve sensing technique performance, since performance is not only tied up to this parameter, but also to the detection-threshold.

In this sense, it is important to investigate the impact of the parameters regarding the Welch method [i.e. the number of segments in which the received data sequence is divided, the number of data points overlapped between consecutive data segments, the number of points considered in the discrete Fourier transforms (DFTs) of individual periodograms] on the performance of ED and identify their trade-off in terms of performance metrics such as probability of detection and probability of false alarm.

In this work, we investigate the performance of the energy detector considering the Welch method for PDS estimation. We derive the test statistic and detection-threshold for ED, as a function of the number of points used in the DFT of individual periodograms and the number of periodograms averaged to determine the PDS estimate. Furthermore, we evaluate the probability of detecting the presence of the primary signal and the probability of missing opportunities for reusing primary spectrum achieved by the detector proposed. The detector presented in this work helps to improve the detection rate without increasing the number of samples collected at the secondary receiver, even in the low SNR regime, which is a critical issue in ED. However, the improvement of the probability of detection comes with the cost of an increased probability of false alarm.

The rest of this paper is structured as follows: in Section 2, we introduce the model considered for spectrum sensing. Section 3 presents the theoretical description of ED in frequency domain using the Welch's periodogram. The analysis of the results obtained by simulations and discussion are presented in Section 4. Finally, we present our conclusions in Section 5.

2 System model and spectrum sensing preliminaries

According to the network model presented in Fig. 1, the SU must identify the presence of an active primary transmitter inside the coverage zone of PU in order to avoid interfering with its transmissions. For this purpose, the SU receives the incoming signal from the radio environment, and then processes it to make a decision regarding the presence of the primary transmitter.

Let $x_c(t)$ be the continuous-time received signal. Assume that we are interested in the frequency band with central frequency f_c and bandwidth B. We sample the received signal at a sampling rate f_s, where $f_s| \geq |B$ in order to yield the discrete representation of received signal $\boldsymbol{x}(n) = x_c(nT_s)$, where $T_s = (1/f_s)$ is the sampling period.

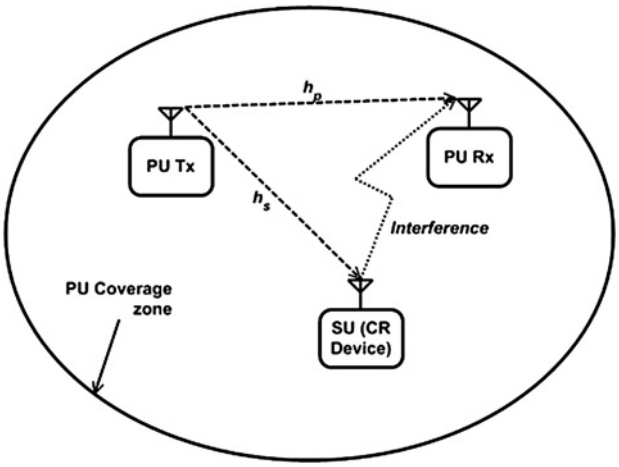

Fig. 1 *Network model considered for spectrum sharing between PUs and SUs*

doi: 10.1049/iet-com.2012.0640

Mathematically, spectrum sensing can be modelled as a binary decision problem [20], where H_0 and H_1 represent primary signal absent and primary signal present, respectively. In terms of the signal received at secondary receiver, H_0 and H_1 are described as

$$H_0: \quad \boldsymbol{x}(n) = \boldsymbol{\eta}(n) \tag{1}$$

$$H_1: \quad \boldsymbol{x}(n) = \boldsymbol{s}(n) + \boldsymbol{\eta}(n) \tag{2}$$

$$n = 0,\ 1,\ \ldots,\ N-1$$

$\boldsymbol{\eta}(n)$ corresponds to the noise, considered as zero-mean complex additive white Gaussian noise, with variance σ_η^2. $\boldsymbol{s}(n)$ is the signal transmitted by PU, considering possible effects of communication channel. Without loss of generality, $\boldsymbol{s}(n)$ is modelled as

$$\boldsymbol{s}(n) = \sum_{l=0}^{q_s} h_s(l)\tilde{\boldsymbol{s}}(n-l) \tag{3}$$

$\tilde{\boldsymbol{s}}(n)$ represents signal transmitted by primary transmitter, $h_s(n)$ models the channel between primary transmitter and secondary receiver, and q_s is the order of channel $h_s(n)$.

The task of a spectrum sensor is to decide whether the observation set $\boldsymbol{x}(n)$, $n = 0, \ldots, N-1$ was generated under H_0 or H_1. This can be accomplished by first forming a test statistic $\gamma(\boldsymbol{x})$ from the received data set, $\boldsymbol{x}(n)$, and then comparing $\gamma(\boldsymbol{x})$ with a predefined threshold λ, that is

$$\gamma(\boldsymbol{x}) \underset{H_0}{\overset{H_1}{\gtrless}} \lambda \tag{4}$$

The performance of a detector can be quantified in terms of its probability of detection, $P_D = \Pr[\gamma(\boldsymbol{x}) > \lambda;\ H_1]$ and probability of false alarm, $P_{FA} = \Pr[\gamma(\boldsymbol{x}) > \lambda;\ H_0]$. In the context of spectrum sensing, the probability of false alarm measures how likely is that SU misses spectrum opportunities because is oblivious of their existence. The probability of detection measures how protected is the PU from the interference caused by SU's transmissions.

3 ED in frequency domain

For ED, the test statistic γ corresponds to the energy contained in the bandwidth of interest. In this sense, to obtain a high performance, we need to make sure that we have an accurate estimation of the energy, or equivalently, of the power contained in the channel monitored.

The power content over a specified bandwidth can be determined by computing the area under the curve of the PDS. According to Welch, the PDS can be estimated by averaging the set of modified periodograms resulting of the segmentation of a data sequence of finite length. The Welch method will yield an asymptotically unbiased and consistent estimate of the true power density spectrum [19].

The structure of ED considering the Welch method is presented in Fig. 2.

The first step in the method proposed by Welch is to divide data sequence into L segments of length M, allowing

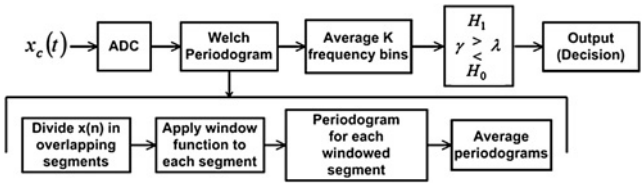

Fig. 2 *Structure of energy detector based on Welch method*

overlapping between successive segments, this is

$$x_i(n) = x(n + iD) \tag{5}$$

$$n = 0,\ 1,\ \ldots,\ M-1$$

$$i = 0,\ 1,\ \ldots,\ L-1$$

where iD is the starting point for the ith segment. The second step is to apply a window function, $w(n)$, to each of the L segments. Then, we compute the periodogram for each sequence

$$\tilde{P}_{xx}^{(i)}(k) = \frac{1}{MU}\left|\sum_{n=0}^{M-1} x_i(n)w(n)e^{-j2\pi(kn/K)}\right|^2, \tag{6}$$

$$i = 0,\ 1,\ \ldots,\ L-1$$

$$k = 0,\ 1,\ \ldots,\ K-1$$

The normalisation factor U ensures that the window function will have unitary power. K corresponds to the number of points considered in the DFT for the periodograms. The values of the individual periodograms obtained from the received signal, $\boldsymbol{x}(n)$, are contained in the matrix of size $L \times K$ defined as

$$\tilde{\boldsymbol{P}}_{xx} \triangleq \left[\ (\boldsymbol{p}_{xx}^{\boldsymbol{1}}) \quad (\boldsymbol{p}_{xx}^{\boldsymbol{2}}) \quad \ldots \quad (\boldsymbol{p}_{xx}^{L})\ \right]^T \tag{7}$$

where superscript T stands for transpose, and vectors $\boldsymbol{p}_{xx}^{\boldsymbol{i}}$ are defined as

$$\tilde{\boldsymbol{p}}_{xx}^{\boldsymbol{i}} \triangleq \left[\ \tilde{P}_{xx}^{(i)}(0) \quad \tilde{P}_{xx}^{(i)}(1) \quad \ldots \quad \tilde{P}_{xx}^{(i)}(K-1)\ \right] \tag{8}$$

The Welch power spectrum estimate corresponds to the average of the L modified periodograms

$$P_{xx}(k) = \frac{1}{L}\sum_{i=0}^{L-1} \tilde{P}_{xx}^{(i)}(k) \tag{9}$$

Or equivalently, in vector form

$$\boldsymbol{p}_{xx} \triangleq \left[\ P_{xx}(0) \quad P_{xx}(1) \quad \ldots \quad P_{xx}(K-1)\ \right] \tag{10}$$

The number of spectral averages (L) used for power estimation can be computed from N, M and D as [19]

$$L = \frac{N-M}{D} + 1 \tag{11}$$

3.1 Test statistic for ED

Making use of (9) to obtain the power content over the frequency bins of interest, we can define the test statistic as

$$\gamma_f = \sum_{k=0}^{K-1} f_K P_{xx}(k) \tag{12}$$

Where $f_K = (W/K)$ corresponds to the frequency resolution selected. From (9) and (12), it is easy to note that γ_f corresponds to the sum of $L \times K$ squared random variables. Assuming that the elements of $\boldsymbol{x}(n)$ are drawn from a Gaussian process, then the elements of its Fourier transform are also Gaussian random variables, since the Fourier transform is a linear operation. In this sense, is possible to state that γ_f follows a central and non-central chi square distribution with LK degrees of freedom, for H_0 and H_1, respectively.

If we assume that the product of $L \times K$ is large enough (>250) to apply the central limit theorem [15], γ_f can be approximated by the Gaussian distribution. In this case, γ_f is normally distributed, with mean and variance as follows

$$\gamma_{f|H_0} \sim N\left(\sigma_\eta^2,\ \frac{2}{LK}\sigma_\eta^4\right) \tag{13}$$

$$\gamma_{f|H_1} \sim N\left((\sigma_s^2 + \sigma_\eta^2),\ \frac{2}{LK}(\sigma_s^2 + \sigma_\eta^2)^2\right) \tag{14}$$

here σ_s^2 corresponds to the power of primary signal, and σ_η^2 is as described in Section 2.

The probability of false alarm and the probability of detection for the energy detector can be defined from the cumulative distribution function (CDF) of γ_f as

$$\begin{aligned} P_{FA} &= \Pr\left(\gamma_{f|H_0} > \lambda\right) = 1 - \Phi_{H_0}(\lambda) \\ &= Q\left(\frac{\lambda - \sigma_\eta^2}{\sqrt{(2/LK)\sigma_\eta^4}}\right) \end{aligned} \tag{15}$$

$$\begin{aligned} P_D &= \Pr\left(\gamma_{f|H_1} > \lambda\right) = 1 - \Phi_{H_1}(\lambda) \\ &= Q\left(\frac{\lambda - \left(\sigma_s^2 + \sigma_\eta^2\right)}{\sqrt{(2/LK)\left(\sigma_s^2 + \sigma_\eta^2\right)^2}}\right) \end{aligned} \tag{16}$$

where λ is the detection-threshold, $\Phi_{H_0}(\lambda)$ and $\Phi_{H_1}(\lambda)$ correspond to the CDF of γ_f under H_0 and H_1, respectively and $Q(\cdot)$ stands for the Gaussian Q-function.

3.2 Detection-threshold

The Neyman-Pearson criterion states that we can construct a decision rule that maximises P_D, constrained to a fixed value of P_{FA} [20]. From (16), we can note that to maximise P_D is necessary to know σ_s^2, and therefore h_S. However for the SU, this knowledge is often neither available nor easy to obtain. In this sense, we opt for maintaining a constant false alarm rate, and without taking into account the P_D, it is possible to set detection-threshold based only on the distribution of the test statistic under H_0. Therefore from (15) the detection-threshold is derived as

$$\lambda = \sigma_\eta^2\left(1 + \sqrt{\frac{2}{LK}}Q^{-1}(P_{FA})\right) \tag{17}$$

The exact noise power is difficult to know, particularly if the SU changes continuously its radio environment. In order to determine detection-threshold, the SU can estimate noise variance from the samples collected to perform spectrum sensing. Nevertheless, noise variance estimation is beyond the scope of this paper, and therefore we assume that the SU performs a preliminary characterisation of the expected value for the noise power, and this value is considered to set λ as in [21].

4 Analysis of results

The results presented in this section correspond to the performance of the energy detector obtained by varying the parameters M (length of subsegments), K (number of points in the DFT and L (number of resulting averages) of the Welch method.

A baseband quadrature phase shift keying (QPSK) modulated signal, with 1.4 MHz of bandwidth is considered as primary signal. The signal is filtered with a root raise cosine filter for pulse shaping, with oversampling factor of 16 samples per transmitted symbol. The received signal is corrupted with receiver noise and the communication channel between primary transmitter and secondary receiver is considered as constant and memory less during each sensing interval, that is, only the line of sight component of the transmitted signal is considered at the receiver end ($q_s = 0$), thus attenuation is attributed only to path loss. In order to determine the performance of the approach under different SNR conditions, we vary the amount of attenuation of the received signal. SNR values considered range from −14 to −20 dB.

For our simulations, we considered a fixed value of $N =$ 5120 samples of the received signal to perform spectrum sensing. The length of subsegments (M) varies from 128 to 1024 points, and the number of points in the DFT equals to the number of samples contained in each subsegment, that is, $K = M$. Overlapping rates [or $= 1 - (D/M)$] vary from 0 to 99% for each value of M. According to the values for N, M and D considered, and from (11), the number of resulting averages (L) spans from 5 to 4993. Performance curves were obtained by Monte Carlo realisations (for each realisation independent random noise and random primary signals are generated) and results are averaged over 1000 realisations.

The product of L for K (LK) parameterises the distribution of the test statistic. This is a reasonable assumption, since this product corresponds to the number of elements on the matrix defined by (7), and used to figure out γ_f. The estimate of the test statistic converges asymptotically to the true value of the energy present, that is $\sigma_\gamma^2 \to 0$ as $LK \to \infty$, where σ_γ^2 corresponds to the variance of the test statistic. When the variance of the test statistic is approximately zero, it is reasonable to limit the value of the detection-threshold within a small interval, because we expect that the estimate of the energy received corresponds to the true energy received. This reasoning is better explained with the help of Fig. 3.

In Fig. 3, we observe the detection-threshold value selected according to (17) normalised to σ_η^2, as a function of the product LK, for different values of P_{FA}. At the minimum value of LK, which corresponds to the number of samples

doi: 10.1049/iet-com.2012.0640

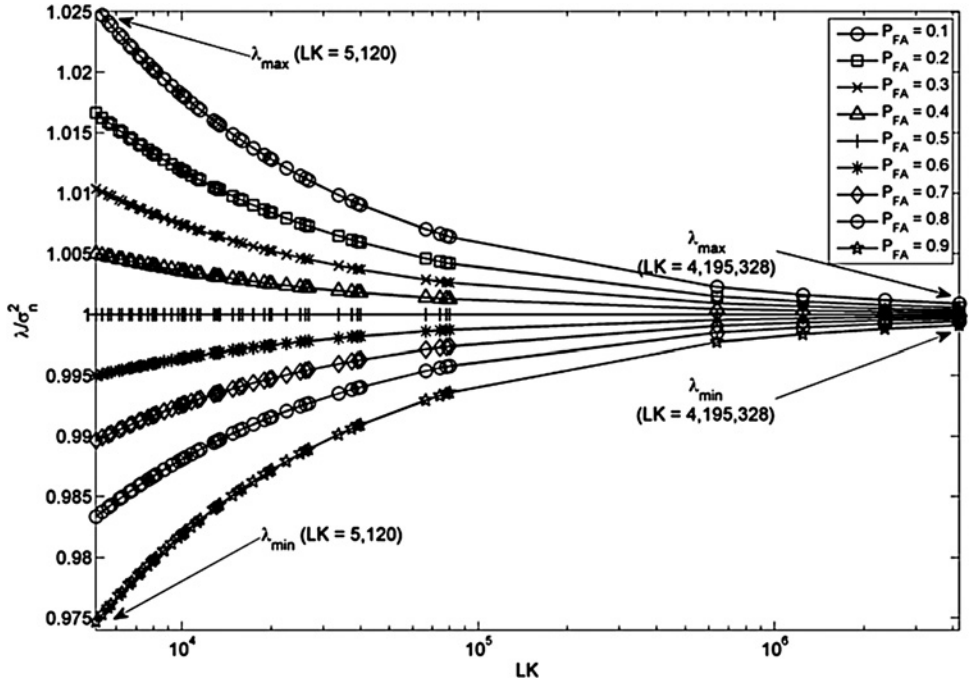

Fig. 3 *Detection-threshold values obtained as a function of the product LK, for different values of P_{FA}*

collected N, we have the maximum variation between the minimum and the maximum possible values for λ. However, as the product LK increases, the range of values obtained for λ is reduced. For the maximum value of $LK =$ 4 195 328, we have that λ ranges from 0.9991 to 1.0009. This means that for an increased number of periodograms averaged, or for an increase of the number of points in the DFT, we can restrict the possible values for λ within a small interval because we expect to have a better estimate of the energy present.

The receiver operational characteristic (ROC) curves for the energy detector operating at SNR = −14 and −20 dB are

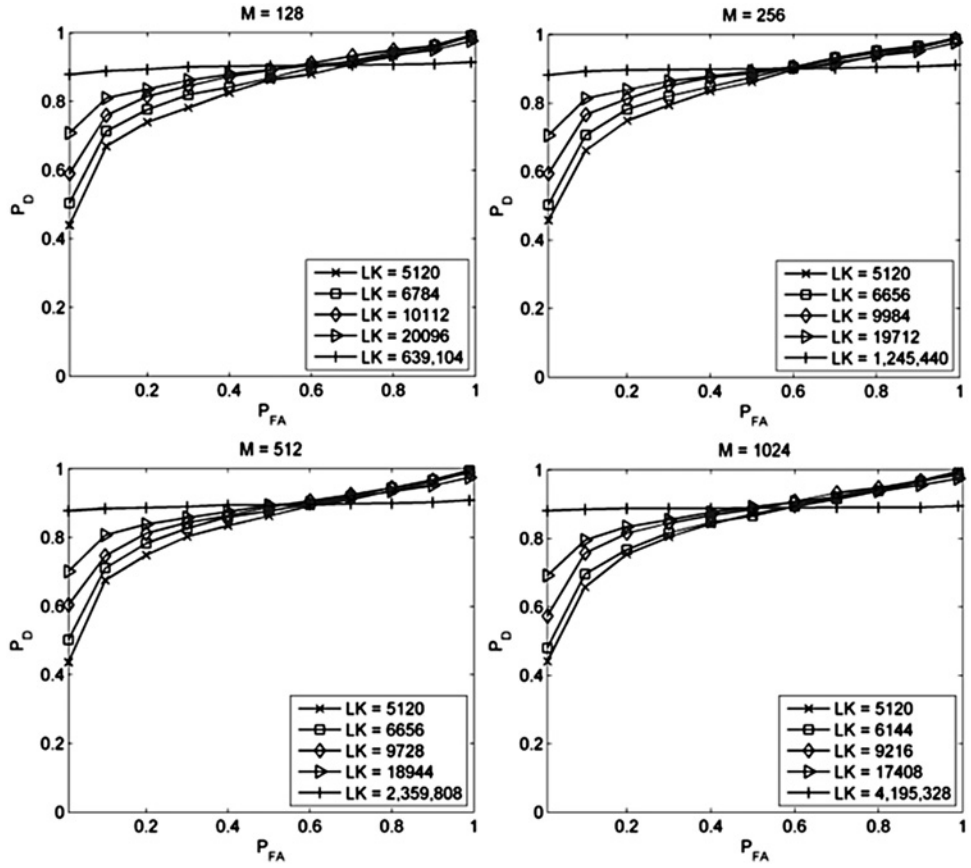

Fig. 4 *ROC curves for the energy detector considering LK in the determination of detection-threshold, SNR = −14 dB*

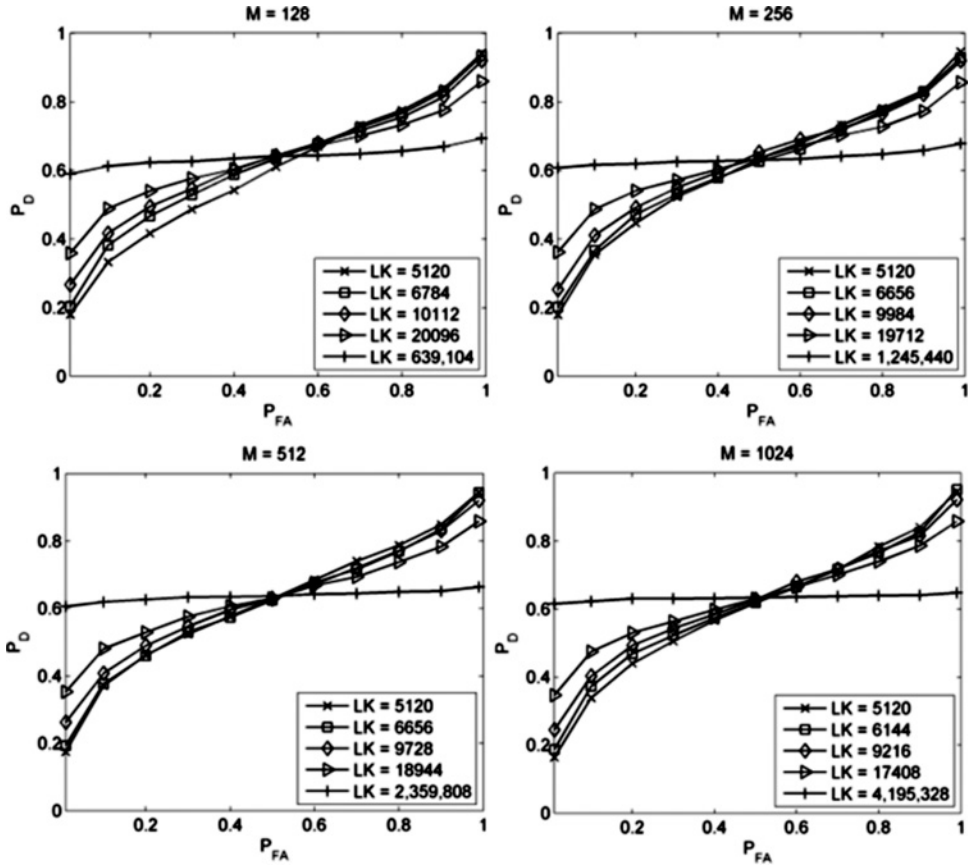

Fig. 5 *ROC curves for the energy detector considering LK in the determination of detection-threshold, SNR = −20 dB*

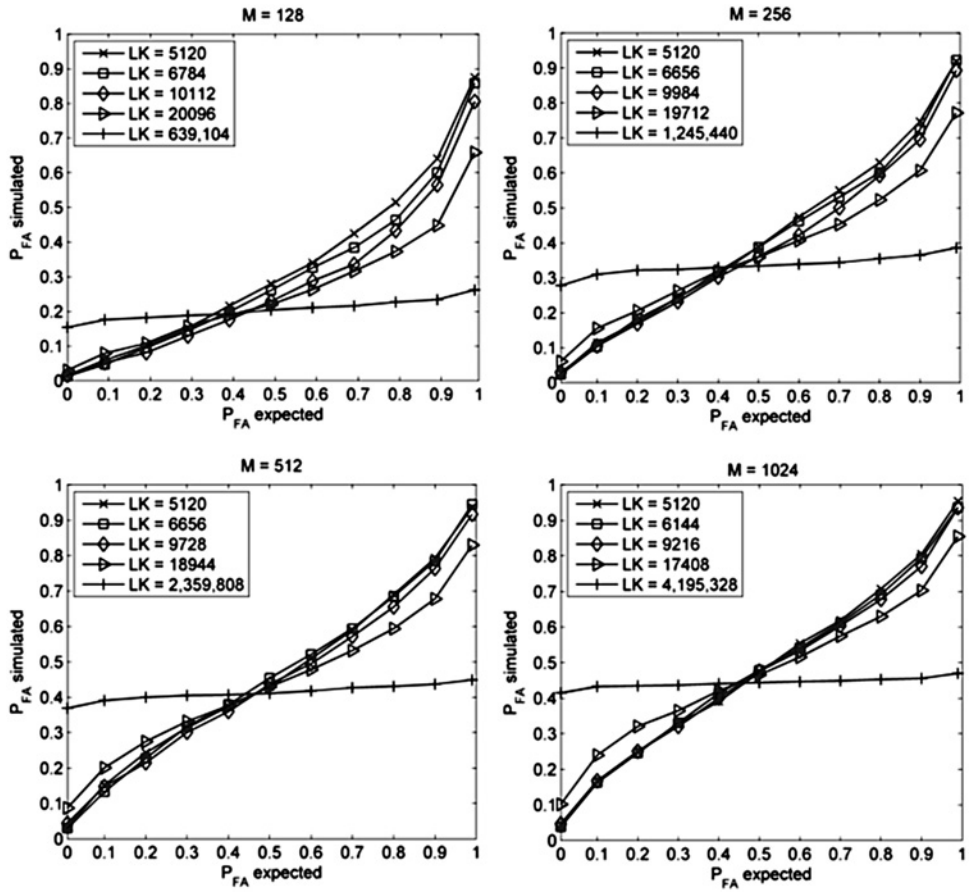

Fig. 6 *Probability of false alarm obtained by simulations because of the election of detection-threshold considering the product LK*

doi: 10.1049/iet-com.2012.0640

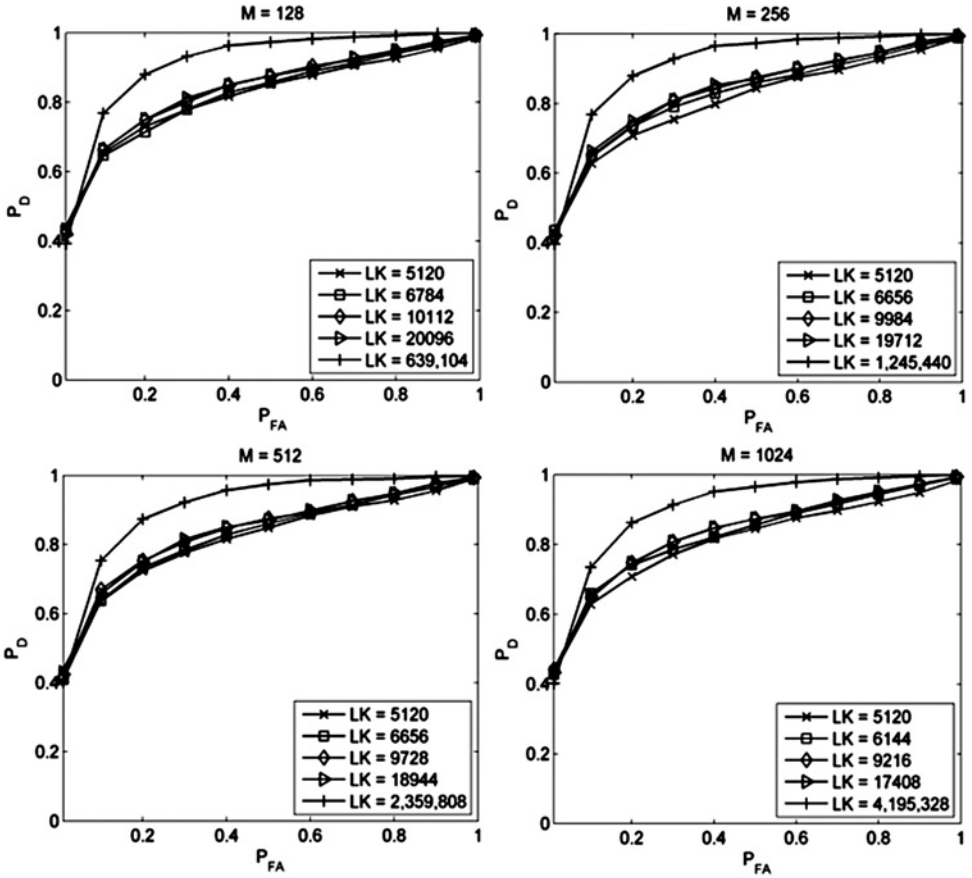

Fig. 7 *ROC curves of the ED considering N in the determination of detection-threshold, SNR = −14 dB*

presented in Figs. 4 and 5, respectively, considering different values of the product LK. ROC curves are commonly used to describe the performance of detection algorithms. The values corresponding to the x-axis of the ROC curve represent the expected probability of false alarm (P_{FA}) as considered for defining λ in (17), and the values of the y-axis correspond to the probability of detection (P_D) obtained by simulations for each value of λ.

We can observe in Figs. 4 and 5 how the P_D is improved by increasing the product LK without the need of increasing the number of samples collected, even in low SNR conditions, and particularly in the low P_{FA} region, that is $P_{FA} \leq 0.1$, which corresponds to desirable values for the P_{FA}. Furthermore, it can be observed that for larger values of LK, the P_D is almost constant for all the values of P_{FA}. This is because for larger values of LK, the values for λ are selected from a small interval (i.e. less variability is expected), and so the P_D becomes oblivious of the expected P_{FA}.

On the other side, if we select λ from the set of values resulting when $LK \to \infty$, then it is possible that sensing performance in terms of false alarm rate is decreased. This is because if $LK \to \infty$, we expect that $\sigma_\gamma^2 = 0$ and hence the energy estimated corresponds to the true energy present. In this sense, for the case when only noise is present, even small differences between the estimated noise power and the received noise power could indicate the presence of primary signal, raising the false alarm rate. These differences are referred to as noise uncertainty.

For our evaluations, the noise uncertainty considered comes from the error induced by energy estimation, that is, the difference between the energy measured (estimated) and the energy value considered (expected) for determining the detection-threshold. In the curves shown in Fig. 6, a fixed value of $\sigma_\eta^2 = 1$ is considered for determining λ according to (17), and the energy measurements captured during simulation, when only noise is present, ranges between $\tilde{\sigma}^2_{\eta,\,\min} = 0.9036$ and $\tilde{\sigma}^2_{\eta,\,\max} = 1.1066$. According to the model presented in [9], the noise uncertainty present in our results is $\rho = 0.44$ dB. Adding other sources of noise uncertainty, for example, occasional interference caused by other secondary transmitters, would increase the rate of false alarms, because of the increase on the variability of the energy estimate.

In Fig. 6, it can be observed that the P_{FA} obtained by simulations becomes greater than the P_{FA} expected as the value of LK increases, particularly when $P_{FA} \leq 0.5$, and $M \geq 256$ samples. In practice, there exist variations in the expected noise power at time of detection, and even though SUs can accurately estimate the energy level present in the channel during the sensing process, the performance of the energy detector will be reduced if the values of λ are not estimated following the variations of the noise power.

Figs. 7 and 8 present ROC curves obtained for the ED when λ is set considering the number of samples collected N instead of product LK as before. From Fig. 7, we can observe that the P_D is not significantly improved as the value of LK increases, except for the largest value of LK obtained for each subsegment length, and from Fig. 8, we can note that the P_D is only improved for the largest value of LK and for $P_{FA} \geq 0.3$. From the results shown in Figs. 7 and 8, we can conclude that reducing the variance on the estimated energy level by increasing the number of averages improves the detection rate for desired values of

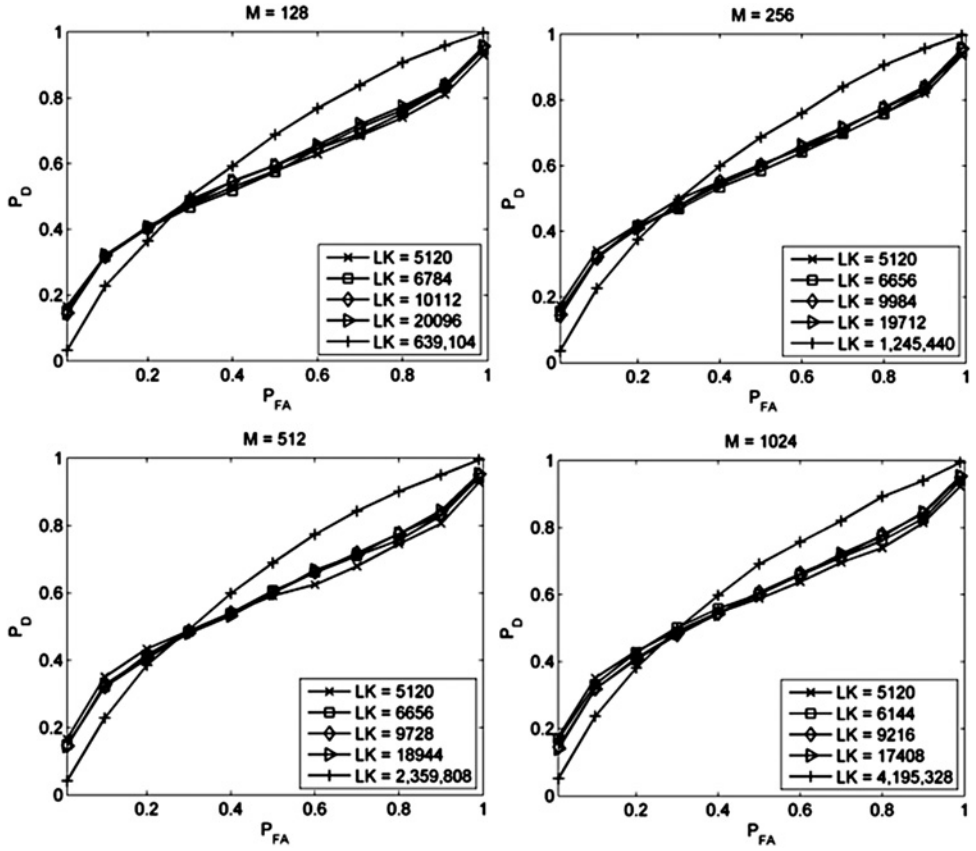

Fig. 8 *ROC curves of the ED considering N in the determination of detection-threshold, SNR = −20 dB*

P_{FA} and low values of SNR, as long as we set λ accordingly to the variance of the noise power.

5 Conclusions

In this work, we presented the evaluation of the ED implemented in frequency domain by using the Welch's method for estimation of the power density spectrum.

In the results presented, we pointed out how the number of averages considered for the power density spectrum estimation and the number of points utilised to compute the DFT in the Welch method have an impact on the performance of the energy detector. We identified that if both parameters are included in the distribution of the test statistic employed to detect the presence of the primary signal, it is possible to improve detection performance. However, in the presence of uncertainty on the noise power, the improvement on the probability of detection will come at the expense of an increased probability of false alarm.

With the approach presented in this work it is possible to increment the probability of detection for a given and low SNR, without increasing the number of samples collected from the observed signal. However, in order to maintain a constant probability of false alarm, accurate techniques for noise variance estimation are needed, because the detection-threshold value is highly dependent on the noise power present at each sensing interval.

From implementation point of view, to increase the value of *LK*, it is needed to increase either the number of points in the DFT, or the number of averages for the PDS estimate. So, it will require more computational resources and an increased processing time. Also, the design of pipelined digital signal processors to compute a higher quantity of periodograms in a determined time interval leads to higher hardware/computational complexity.

6 References

1 General survey of radio frequency bands – 30 MHz to 3 GHz. Vienna, VA: shared spectrum company, 2010. Report no. 20100323

2 Erpek, T., Steadman, K., Jones, D.: 'Dublin Ireland – spectrum occupancy measurements' (Shared Spectrum Company, 2007)

3 Haykin, S.: 'Cognitive radio: brain-empowered wireless communications', *IEEE J. Sel. Areas Commun.*, 2005, **23**, (2), pp. 201–220

4 Tandra, R., Sahai, A., Mishra, S.M.: 'What is a spectrum hole and what does it take to recognize one?', *Proc. IEEE*, 2009, **97**, (5), pp. 824–848

5 Yucek, T., Arslan, H.: 'A survey of spectrum sensing algorithms for cognitive radio applications', *IEEE Commun. Surv. Tutor.*, 2009, **11**, (1), pp. 116–30

6 Sutton, P.D., Nolan, K.E., Doyle, L.E.: 'Cyclostationary signatures in practical cognitive radio applications', *IEEE J. Sel. Areas Commun.*, 2008, **26**, (1), pp. 13–24

7 Urkowitz, H.: 'Energy detection of unknown deterministic signals', *Proc. IEEE*, 1967, **55**, (4), pp. 523–531

8 Pawelczak, P., Nolan, K., Doyle, L., Oh, S.W., Cabric, D.: 'Cognitive radio: ten years of experimentation and development', *IEEE Commun. Mag.*, 2011, **49**, (3), pp. 90–100

9 Tandra, R., Sahai, A.: 'Fundamental limits on detection in low SNR under noise uncertainty'. Proc. Conf. Wireless Networks, Communications and Mobile Computing, Maui, HI, USA, June 2005, vol. 1, pp. 464–469

10 Zeng, Y., Liang, Y.: 'Eigenvalue-based spectrum sensing algorithms for cognitive radio', *IEEE Trans. Commun.*, 2009, **57**, (6), pp. 1784–1793

11 Pillay, N., Xu, H.J.: 'Blind eigenvalue-based spectrum sensing for cognitive radio networks', *IET Commun.*, 2012, **6**, (11), pp. 1388–1396

12 Sato, T., Umehira, M.: 'A new spectrum sensing scheme using overlap FFT filter-bank for dynamic spectrum access'. Proc. Int. Conf. Cognitive Radio Oriented Wireless Networks and Communications (CROWNCOM), Osaka, Japan, June 2011, pp. 6–10

13 Ma, J., Li, G.Y., Juang, B.H.: 'Signal processing in cognitive radio', *Proc. IEEE*, 2009, **97**, (5), pp. 805–823

doi: 10.1049/iet-com.2012.0640

14 Proakis, J.G., Manolakis, D.G.: 'Digital signal processing. Principles, algorithms and applications' (Pearson Education, 2009, 4th edn.)
15 Cabric, D., Tkachenko, A., Brodersen, R.W.: 'Experimental study of spectrum sensing based on energy detection and network cooperation'. Proc. First Int. Workshop on Technology and Policy for Accessing Spectrum, Boston, MA, USA, June 2006, Article no. 12
16 Gismalla, E.H., Alsusa, E.: 'Performance analysis of the periodogram-based energy detector in fading channels', *IEEE Trans. Signal Process.*, 2011, **59**, (8), pp. 3712–3721
17 Sarvanko, H., Mustonen, M., Hekkala, A., Mammela, A., Matinmikko, M., Katz, M.: 'Cooperative and noncooperative spectrum sensing techniques using Welch's periodogram in cognitive radios'. Proc. First Int. Workshop on Cognitive Radio and Advanced Spectrum Management (CogART), Aalborg, Denmark, February 2008, pp. 1–5
18 Matinmikko, M., Sarvanko, H., Mustonen, M., Mammela, A.: 'Performance of spectrum sensing using Welch's periodogram in Rayleigh fading channel'. Proc. Fourth Int. Conf. Cognitive Radio Oriented Wireless Networks and Communications (CROWNCOM), Hannover, Germany, June 2009, pp. 1–5
19 Welch, P.: 'The use of fast Fourier transform for the estimation of power spectra: a method based on time averaging over short, modified periodograms', *IEEE Trans. Audio Electroacoust.*, 1967, **15**, (2), pp. 70–73
20 Kay, S.M.: 'Fundamentals of statistical signal processing: detection theory' (Prentice-Hall, 1998, 1st edn.)
21 Shellhammer, S.J., Sai Shankar, N., Tandra, R., Tomcik, J.: 'Performance of power detector sensors of DTV signals in IEEE 802.22 WRANs'. Proc. First Int. Workshop on Technology and Policy for Accessing Spectrum, Boston, MA, USA, June 2006, Article no. 4